DELIVERABLE REPORT

WP7 JRA2 – Research on High Precision Manufacturing

D7.14

Test of re-alignment of nanostructures in synchrotron experiment by in-situ marker deposition

Expected date

M36

NFFA-Europe has received funding from the EU's H2020 framework programme for research and innovation under

nffa.eu

PROJECT DETAILS

PROJECT ACRONYM	PROJECT TITLE
NFFA-Europe	NANOSCIENCE FOUNDRIES AND FINE ANALYSIS - EUROPE
GRANT AGREEMENT NO:	FUNDING SCHEME
654360	RIA - Research and Innovation action
START DATE	
01/09/2015	

WP DETAILS

WORK PACKAGE ID	WORK PACKAGE TITLE
WP7	JRA2 – Research on High Precision Manufacturing

WORK PACKAGE LEADER

Christian David (PSI)

DELIVERABLE DETAILS

DELIVERABLE ID	DELIVERABLE TITLE
D7.14	Test of re-alignment of nanostructures in synchrotron experiment by in-situ marker deposition

DELIVERABLE DESCRIPTION

This deliverable report describes the in-situ marker-supported nano-transfer of single nano-objects from nanoscience instrument to focused X-ray beamlines

EXPECTED DATE	ESTIMATED INDICATIVE PERSONMONTHS
M36 31/08/2018	MM

AUTHOR(S)

Christoph Seitz, Satishkumar Kulkarni, Thomas F. Keller

PERSON RESPONSIBLE FOR THE DELIVERABLE

Christian David (PSI)

NATURE

P - Prototype

DISSEMINATION LEVEL

- ☒ P - Public
- ☐ PP - Restricted to other programme participants & EC: (Specify)
- ☐ RE - Restricted to a group (Specify)
- ☐ CO - Confidential, only for members of the consortium

REPORT DETAILS

ACTUAL SUBMISSION DATE	NUMBER OF PAGES
06/09/2018 hh.mm AM	**12**

FOR MORE INFO PLEASE CONTACT

Thomas F. Keller Tel. +49 40 8998-6010 Email: Thomas.Keller@DESY.de

Version	Date	Author(s)	Description / Reason for modification	Status
0	06/08/2018	Thomas F. Keller		Draft
1	15/08/2018	C. Seitz		Update
2	20/08/2018	Thomas F. Keller		Update
3	22/08/2018	Benedikt Rösner		Final
				Choose an item.

Contents

Executive Summary

This deliverable report D7.14 is part of the overall development of a protocol to enable the reliable re-alignment of nanostructures in synchrotron experiments by in-situ marker deposition. Here, we specifically report on the activities within the subtask of the Joint Research Action JRA2 “High Precision Manufacturing” with the aim to create and employ well defined markers in terms of the marker position on a sample, the marker size, and the optimal marker thickness. The re-alignment protocol developed within the Joint Research Action JRA5 “Advanced Nano-Object Transfer and Positioning” requires an in-situ deposition of markers in order to create the markers in close vicinity to the region of interest containing the nano-objects.

In particular, we applied ion- (IBID) and electron- (EBID) beam induced deposition in a dual beam focused ion beam instrument (FIB-SEM) to create Pt based markers from a metal-organic precursor with systematically varied system parameters like, e.g., the spot- or beam-size of the electron or ion beam, as well as the electron or ion beam energy, and determined the resulting thickness by atomic force microscopy (AFM). Based on our results we conclude that with the here applied settings, it is possible to reliably create markers for re-localization with nanometre precision, provided a careful calibration is carried out. Moreover, it is not only possible to provide markers for wide range of thicknesses and applications, but also marker thicknesses outside the tested parameter range by extrapolating and adjusting the writing time.

As such, we developed a protocol based on the IBID/EBID technique to produce in-situ fabrication of alignment markers. Along with the concepts, software protocols and hardware implementations for a hierarchical marker arrangement developed within the Joint Research Action JRA5, the outcome of this JRA2 deliverable report permits a well-defined nano-transfer between nanoscience instruments and focused X-ray beamlines that is already by now offered to NFFA user requests within the category “Lithography and Patterning”. The report also stresses the strength and the fruitful cross-JRA interactions between the technical developments pushed forwarded within JRA2 and JRA5.

1. Concept

This deliverable report D7.14 describes tested processing parameters that can be utilized to reproducibly write IBID/EBID markers within a given thickness range between a few and around 200 nanometers. It is strongly related to parallel developments within JRA5, which strongly relies on the outcome described within this report D7.14: Aspects dealing with the overall development of a Nano-Transfer protocol within JRA5 are summarized in the related deliverable reports D10.1: “Software routine for coordinate definition and relocation of single nano-objects”, and D10.2: “Implementation of transfer and positioning system at nanolabs and ALSFs” covering complementary steps needed to assist nano-science users to re-locate their pre-selected region of interest containing a nanoscale object under investigation like, e.g., a single nanoparticle, a single nanowire or quantum dot. Before the outcome of this D7.14 come into play, a “marker design on demand” is required to develop the optimal arrangement of hierarchical markers on a given sample, the lateral marker size for each hierarchy level, and finally, the optimal marker thickness. With a known target thickness for each of the markers, appropriate processing parameters can be chosen from the values reported in this deliverable report D7.14.

We established a workflow to create standardized markers for the in-situ marker deposition by IBID/EBID from a platinum precursor on selected sites on top of a sample surface. These results along with all informations provided within the deliverable reports D10.1 and D10.2 serves as a platform to offer transnational user access not only to a combined nano-instrumentation and X-ray analysis environment but at the same time supporting their novel nanoscience experiments with a guided nano-transfer and re-positioning.

2. Design specification

Different marker thicknesses are required for different applications. First, for a coarse re-localization in the focused X-ray beam thick markers are useful to ensure a large intensity and permitting low counting times for the marker search. In particular, zero order hierarchical markers located on well specified sample regions like close to the sample edges should have a large lateral size and thickness. Higher order hierarchical markers will be stepwise located closer to the region of interest and will be therefore smaller in size as well as thickness to avoid contaminations in the analysis region that could potentially affect the results of the experiment.

Second, different marker localization schemes require different marker thicknesses. For X-ray fluorescence, being very sensitive, only 10 nm thick markers are usually sufficient to ensure an easy identification while scanning the sample through the X-ray beam. For the here applied Pt based markers created from a Pt precursor material, usually the Pt L_3 edge is used to locate the Pt inside the marker. Another detection scheme, exploiting the nano-crystalline structure of the marker material, requires a typical marker thickness of 100 nm: A 100 nm thick Pt based IBID/EBID marker can be located using, e.g., the Pt(111) Bragg peak signal while scanning the sample. Already these considerations indicate the existence of an optimal marker thickness for different searching and localization mechanisms: For the X-fluorescence thin markers are sufficient but require X-ray energy above the Pt L_3 edge, i.e. around 12 keV. On the other hand, localization via the Pt Bragg peak requires around one order of magnitude thicker markers, but can be used at all relevant X-ray energies, in particular around 8-9 keV, well below the Pt L_3 edge, where the often used compound refractive lenses (CRLs) focusing optics are most efficient and provide the most intense and brilliant beam on the sample.

For post-analysis by AFM, often 1-2 nm thick markers are already sufficient provided they are written onto an overall flat surface, like, e.g., on an epi-polished single crystal surface. Still, it might be desirable to complement such a highest hierarchical order marker with thicker auxiliary markers in a larger distance to the region of interest that could be located with an attached optical microscope, facilitating an overall easier and faster nano-transfer.

Fig. 1 shows an outline of the design of this study, indicating the varied parameters and the applied settings for each of the markers. Varied parameters include the acceleration voltage that was varied from 5-20 keV and critically affects the cross-section for interaction of the probe (ions or electrons) with the precursor molecule. It indicates the probability that the probe breaks up the Pt containing molecule such that hydrocarbon segments remain in the gas phase inside the vacuum and are pumped away, whereas the Pt containing residue is absorbed onto the surface in the dedicated marker region. Furthermore, the spot-size, i.e. a measure of the diameter of the beam defining aperture, is an indicator for the ion or electron beam size and the total beam current or intensity, i.e., the number of the ions or electrons in the beam. Finer lines require a higher resolution, compromising lower beam intensity and consequently results in a longer writing time to achieve the

same marker thickness. The setup was designed in a 3x3 array, as shown in Figure 1. A silicon wafer served as test substrate. All pattern where written with the pattern implemented software on a dual-beam FIB SEM instrument at DESY NanoLab [1]. When using the gas injection system a nozzle (see, e.g. Figure 2) is brought into a well defined distance of around 500 µm from the substrate surface in a reproducible way to ensure a controlled deposition and resulting thickness. The nozzle permits to bring the Pt containing precursor molecules in close vicinity to the surface to enhance an efficient EBID deposition.

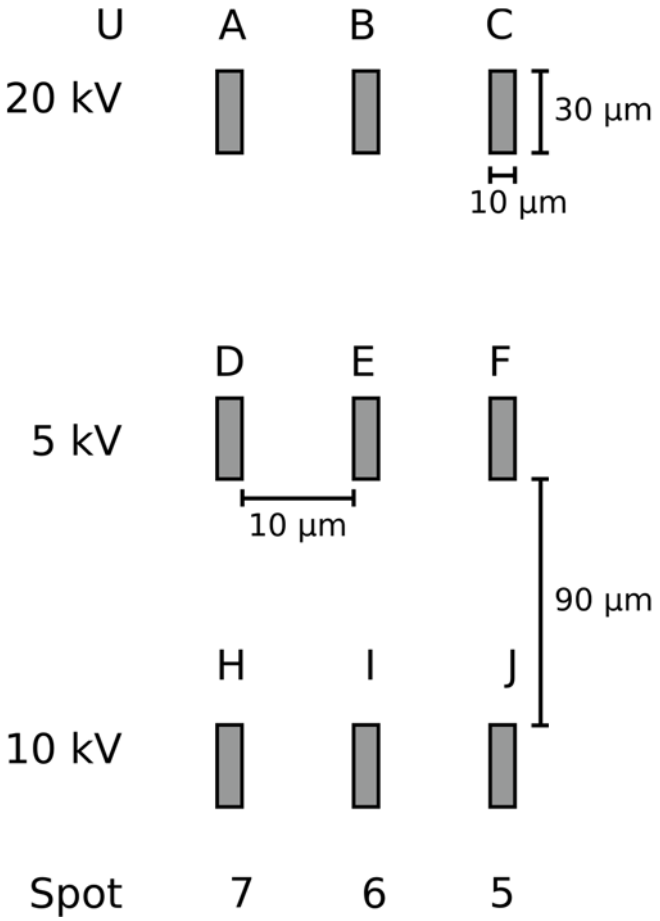

Figure 1: Scheme of marker preparation with different spot sizes and electron acceleration voltages used. All markers are patterned with EBID. (S. Kulkarni, T. F. Keller, DESY)

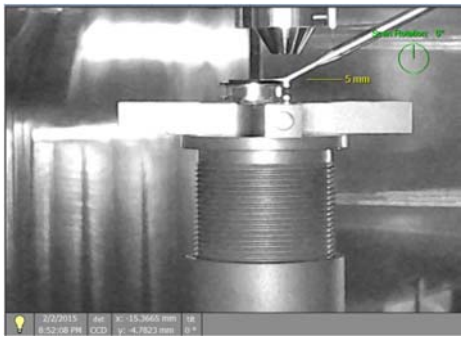

Figure 2: Chamber view inside a FIB /SEM. From top, the pole shoe can be seen, from the bottom the sample is approached towards the optimal working distance of around 5 mm. From the left side, the GIS nozzle is brought in close vicinity to the sample surface to ensure optimal deposition conditions. (S. Kulkarni, T. F. Keller, DESY)

Rows contain markers with different spot-sizes deposited at the same acceleration voltage, i.e. 20 kV, 5 kV and 10 kV. Correspondingly, the three columns contain EBID patterned markers with these different acceleration voltages for A - spot-size 7, B - spot size 6, and C - spot size 5. The marker size is 10 µm × 30 µm and the same for all applied markers. The rows and columns are located 90 µm and 10 µm apart, respectively.

3. Results

3.1 SEM analysis of the EBID marker array

Figure 3 shows an SEM overview image of the array after the EBID deposition of all nine markers. Clearly, all markers (indicated as A, B, C in row 1 for 20 kV; D, E, F in row 2 for 5 kV and H, I, J in row 3 for 10 kV) can be identified by their contrast in the secondary electron detector image and their lateral size. The lateral dimensions agree well with the values specified in the patterning software. Apparent is the varying contrast of all markers arising from the resulting thicknesses obtained by the applied process and deposition parameters.

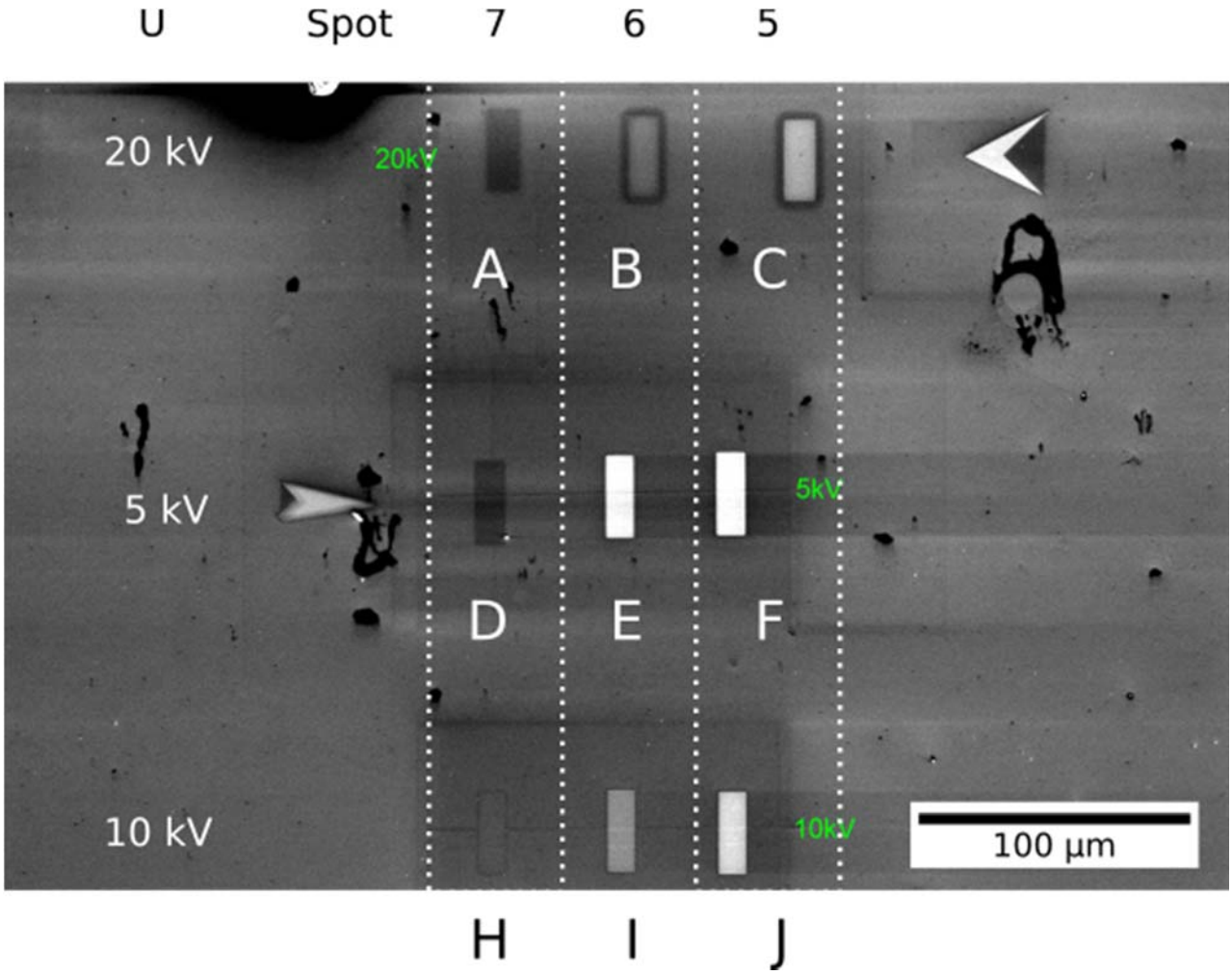

Figure 3: Secondary electron image of the deposited Pt markers. All markers are indicated by letters for identification (see, e.g., the main text) Acceleration voltages used are given as overlay inside the SEM image. (S. Kulkarni, T. F. Keller, DESY)

Marker B and C clearly show a small fringe surrounding the main marker. Such a faint frame can also be observed for the markers written at 10 kV, e.g., markers H, I and J, while markers A and D appear with a dark, uniform contrast and markers E and F with a rather bright uniform contrast. The IBID/EBID process is known to create a small and thin halo around the desired pattern, originating from electrons incoherently scattered back from the substrate. Being close to the surface, they collide with the Pt precursor molecules. As they still possess sufficient energy, there is a non-negligible probability to crack the molecules, leading to absorption of residual Pt around the main marker area.

3.2 AFM analysis of the EBID marker array

Figure 4 shows nine separate AFM images of the EBID pattern markers shown in the SEM overview image in Figure 3. As noted from Figure 3, the patterning resulted in the desired lateral marker size of 10 µm × 30 µm. The colour code on the right side of Figure 4 indicates height values, from which the resulting mean marker height values can be deduced for each of the nine markers.

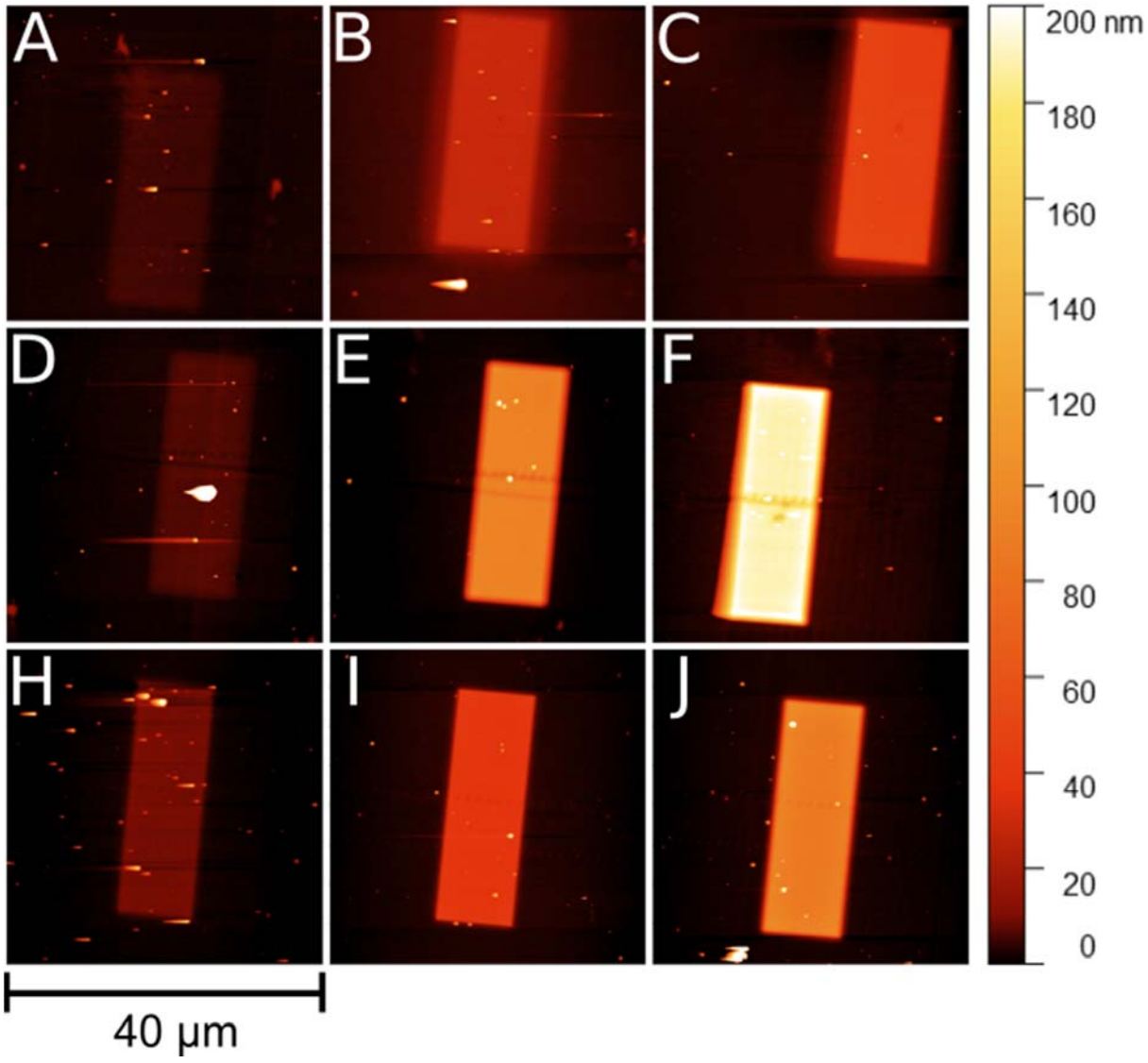

Figure 4: AFM height measurements of the obtained Pt markers, a-c) deposited at 20 kV, d-f at 5 kV, h-j written at 10 kV. Spot-sizes in the left, center and right column are 7, 6 and 5, respectively (C. Seitz, T. F. Keller, DESY).

Obviously, within each row, i.e., for each acceleration voltage, the markers become brighter, i.e., higher, from left to right. That implies that for all acceleration voltages, the thickness increases when the spot-size is decreased from 7 to 5. This could be expected as a smaller spot-size implies a smaller apperture within the column of the ion or electron beam. The apperture reduces the beamsize, leading to a higher possible lateral resolution but also to less intense beam and with respect to the IBID/EBID process, less ions or electrons that could interact with the Pt GIS precursor molecules.

3.3 EBID process parameter dependent marker thickness

Figure 5 shows the corresponding line profiles across the AFM tomography / height images of Figure 4. From Figure 5, the spot size dependence of the resulting marker thicknesses for each acceleration voltage can be quantitatively deduced. The thickest markers are created at an acceleration voltage of 5 kV, and the thinnest markers result from the EBID process at 20 kV. Whereas for spot-size 7 the markers created at 5 kV reach only around 4 nm, with spot-size 5 it reaches around 200 nm, i.e. a factor of 50 more.

Furthermore, the line profiles in Figure 5 permit to analyse the lateral extension and thickness of the halos surrounding some of the markers, as discussed above in section 2.1. It is apparent that the halos are most significant for 20 kV, i.e., in Figure 5 on the top left. This implies that the halo is not scaling with the overall intensity, since at the most efficent Pt deposition at 5 kV, the halo is not even visible, altough the markers have the largest thickness.

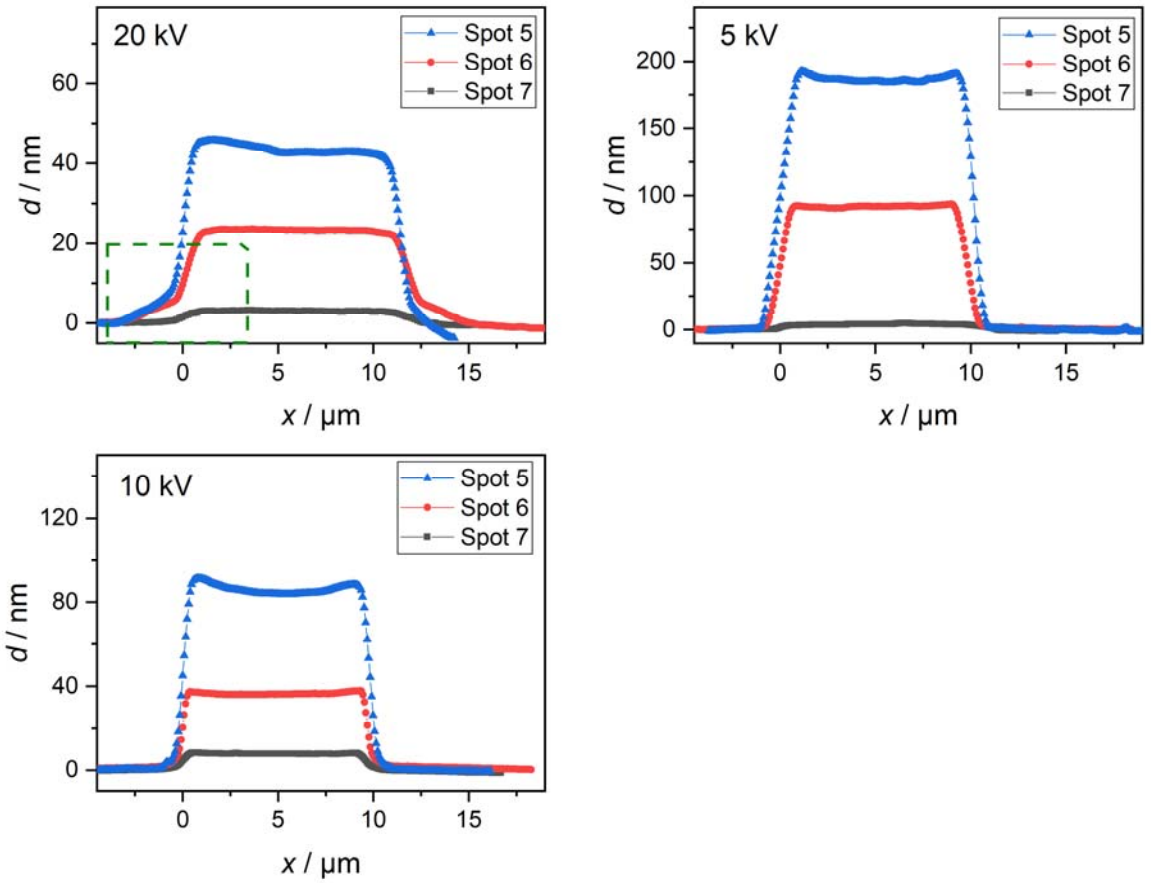

Figure 5: Line profiles of each analyzed Pt marker derived from the AFM measurements in Figure 4, for the acceleration voltages 20 kV (top left), 5 kV (top right) and 10 kV (bottom) for different spot-sizes. (C. Seitz, T. F. Keller, DESY).

Figure 6 summarizes on the left the nominal writing times as calculated by the internal software of the dual beam FIB/SEM instrument. For each spot size, the slopes in the graph indicate the proportionality for each spot-size and accleration voltage (see, e.g., Figure 6 on the left). Except the marker indicated at spot-size 4, taking around 7 h writing time, were written by EBID and subsequently analysed by AFM.

Note that for all 9 tested settings (3 acceleration voltages and for each 3 spot-sizes) the target marker thickness was set to 1 µm. The graph in Figure 6 on the right shows the experimentally determined achieved AFM marker thickness values. Indeed, there are large descrepences from the set value, with the minimum difference of around a factor of 5 less than the target value of 1 µm, i.e. 200 nm obtained for 5 kV and spot-size 5. For all other tested settings, the differences are even larger.

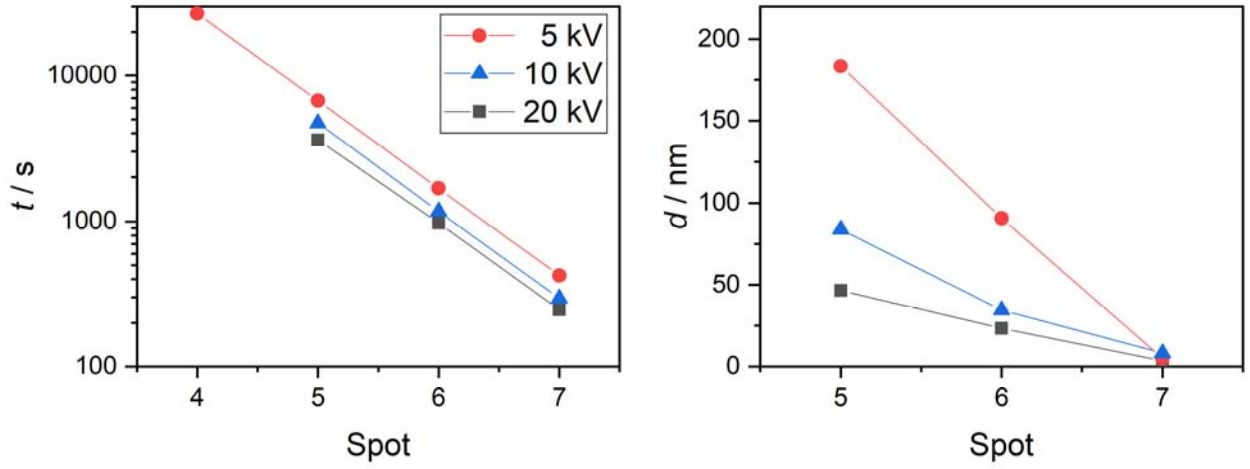

Figure 6: Calculated time required for deposition (t, left) and thickness of resulting marker measured in AFM (d, right) in dependence of the spot-size (C. Seitz, T. F. Keller, DESY).

Still, for a given acceleration time and spot-size, the main systematic trend does hold: With increasing spot size, i.e., smaller beam defining aperture, the resulting thickness of the markers is decreased, indicating the overall mutual dependence and equivalence of smaller spot-size and longer writing time. The graph in Figure 6 on the right clearly shows that the most efficient, i.e., thick markers are created with the smallest spot size and the lowest acceleration voltage.

3.4 Test of re-alignment of nanostructures in synchrotron experiment by in-situ marker deposition

Figure 7 and 8 document that Pt based markers created by e-beam lithography (Figure 7, marker preparation not further described here) and by EBID (Figure 8) can be found with a focused X-ray beam at beamlines P10 at PETRA III and ID01 at ESRF, respectively. The SEM images on the left side of Figures 7 and 8 where obtained with the SEM at DESY NanoLab, whereas the right hand side in Figure 7 was obtained with a silicon drift fluorescence detector (SDD) mounted at beamline P10, while the right hand side of Figure 8 was obtained with a 2D area detector and with a set region of interest in the vicinity of the Pt(111) Bragg peak at ID01.

Both scanning images on the right of Figures 7 and 8 where obtained while scanning the sample through the focused X-ray beam, and the SEM images on the left where obtained by scanning the electron beam across a fixed sample.

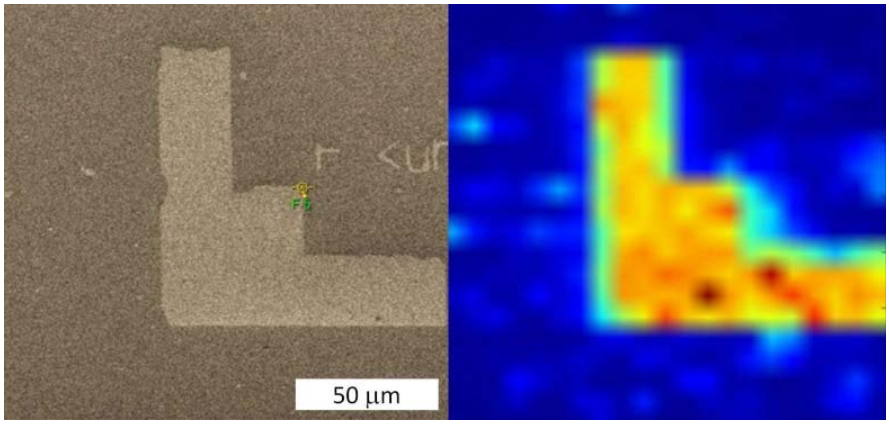

Figure 7: SEM (left) and X-ray fluorescence images (right) at the Pt L_3 edge. The X-ray image was obtained at the coherence beamline P10 at PETRA III, DESY, while scanning the sample through the X-ray beam. For this particular sample, the markers were created by e-beam litoghaphy. The thickness is around 10 nm. (T. F. Keller, R. Shyduk, S. Kulkarni, A. Stierle et al., DESY).

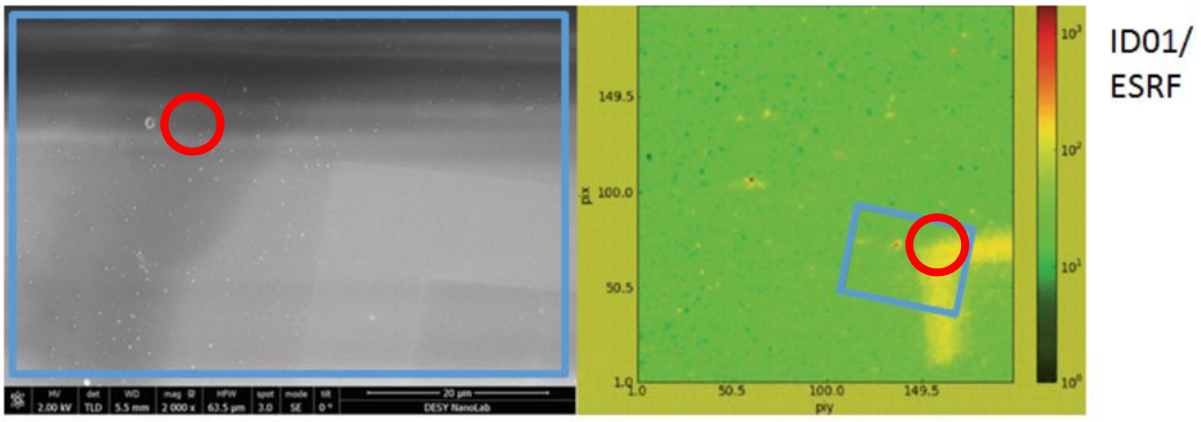

SEM image of STO substrate ROI containing pre-selected nano-object and the ion-beam induced GIS based first hierarchy level Pt marker

X-ray fast scan "K-MAP": 2D plot of the integrated **Pt(111) crystal truncation rod intensity** in the vicinity of the Pt (111) Bragg peak position.

Figure 8: SEM image (left) with a marker and X-ray fast scan "K-MAP" image recorded at beamline ID01 at ESRF, exploiting the Pt(111) intensity of the nanocrystalline Pt based marker and Pt nanoparticles. The image size of the X-ray scanning image on the right is 200 µm. (M. Abuin, T. F. Keller, A. Stierle et al., DESY, M. R. Richard, S. Leake, ESRF, taken from the JRA5 deliverable report D10.2).

At the same time, Figure 8 documents the steps to re-localize a pre-selected nano-region of interest. In this case, the nano region containing a ~100 nm in diameter large isolated Pt single crystal platinum nanoparticle. Both SEM and X-ray scanning image contain at the same time the Pt based markers as well as the region of interest with the nanoparticle, as indicated with the red circles.

This proves the feasibility of the nano-transfer. Indeed, using the applied marker size, thickness and arrangement and the search algorithm developed within JRA5, an operando nano-catalysis experiment could be successfully performed. Even more, the analysed nanoparticle could be re-located back at DESY NanoLab for a post-analysis by SEM and AFM.

4. Conclusions and Perspectives

Within the JRA2 “High Precision Manufacturing” subtask 7.1.2 “Development of 3D lithography techniques”, we analzysed the IBID/EBID deposition of a Pt containing precursor molecule inside a dual beam FIB/SEM instrument to create well defined navigation markers for the JRA5 “Advanced Nano-Object Transfer and Positioning”. As an example, we describe here the results for the test of the EBID process, where the two process parameters spot-size and acceleration voltage was tested by systematic variation. With the here reported results we supply processing parameters to write IBID/EBID based markers in a controlled way onto sample surfaces, and design their lateral arrangement in a hierarchical order, their lateral size and their thickness.

Based on this report it is apparent that a careful choice of EBID deposition parameters need to be selected, and in case a precise thickness is needed for a specific application, a calibration is needed. The descrepancy between the set thickness and the resulting AFM thickness is significant and related to the fact that the internal thickness calculations assumes the IBID process with much higher deposition rates. Indeed, the IBID process results in much better agreement between set and resulting marker thickness. In any case, for both, EBID and IBID a calibration is highly recommended.

Wheras the occurance of a halo surrounding IBID marker structures that scales with the total marker thickness is well known, we also observed a halo for the more sensitive EBID markers at the highest tested accleration voltage of 20 kV. This implies that for clean sample surfaces, where contaminations are detrimental, like for an operando nano-catalysis experiment, EBID should be chosen in the close vicinity of the region of interest, and the accleration voltage should be carefully selected, i.e., by chosing a smaller, high efficient beam energy of 5 kV.

Overall, this is an integral part of the offer of a nano-transfer package that has already turned into “a new offer” which can be requested by NFFA transnational acess nanoscience users from the NFFA webpage during proposal submission (see, e.g.: https://www.nffa.eu/offer/lithography-patterning/installation-1/nano-object-transfer-positioning/).

Already now this work has facilitated a significant advance in understanding nanoscale processes, e.g., by in-situ or operando tracking the structural dynamics of single nano-objects, and has been requested within the nano-transfer within recently submitted NFFA user proposals.

References

[1] *Stierle, A.; Keller, T. F.; Noei, H.; Vonk, V.; Roehlsberger, R. DESY NanoLab. J. large-scale Res. Facil. JLSRF* ***2016****, 2, A76*.